

# A Set of Organelle-Localizable Reactive Molecules for Mitochondrial Chemical Proteomics in Living Cells and Brain Tissues

Yuki Yasueda,<sup>†</sup> Tomonori Tamura,<sup>†</sup> Alma Fujisawa,<sup>†</sup> Keiko Kuwata,<sup>‡</sup> Shinya Tsukiji,<sup>§,||</sup> Shigeki Kiyonaka,<sup>†</sup> and Itaru Hamachi<sup>\*,†,⊥</sup>

<sup>†</sup>Department of Synthetic Chemistry and Biological Chemistry, Graduate School of Engineering, Kyoto University, Katsura, Nishikyo-ku, Kyoto, 615-8510, Japan

<sup>‡</sup>Institute of Transformative Bio-Molecules (ITbM), Nagoya University, Chikusa, Nagoya, 464-8602, Japan

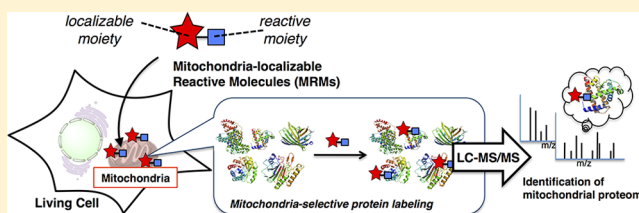
<sup>§</sup>Frontier Research Institute for Materials Science (FRIMS), Nagoya Institute of Technology, Gokiso-cho, Showa-ku, Nagoya, 466-8555, Japan

<sup>||</sup>Department of Life Science and Applied Chemistry, Department of Nanopharmaceutical Sciences, Nagoya Institute of Technology, Gokiso-cho, Showa-ku, Nagoya, 466-8555, Japan

<sup>⊥</sup>CREST (Core Research for Evolutional Science and Technology, JST), Sanbancho, Chiyodaku, Tokyo, 102-0075, Japan

## S Supporting Information

**ABSTRACT:** Protein functions are tightly regulated by their subcellular localization in live cells, and quantitative evaluation of dynamically altered proteomes in each organelle should provide valuable information. Here, we describe a novel method for organelle-focused chemical proteomics using spatially limited reactions. In this work, mitochondria-localizable reactive molecules (MRMs) were designed that penetrate biomembranes and spontaneously concentrate in mitochondria, where protein labeling is facilitated by the condensation effect. The combination of this selective labeling and liquid chromatography–mass spectrometry (LC–MS) based proteomics technology facilitated identification of mitochondrial proteomes and the profile of the intrinsic reactivity of amino acids tethered to proteins expressed in live cultured cells, primary neurons and brain slices. Furthermore, quantitative profiling of mitochondrial proteins whose expression levels change significantly during an oxidant-induced apoptotic process was performed by combination of this MRMs-based method with a standard quantitative MS technique (SILAC: stable isotope labeling by amino acids in cell culture). The use of a set of MRMs represents a powerful tool for chemical proteomics to elucidate mitochondria-associated biological events and diseases.



## INTRODUCTION

Proteome analysis relying on advanced mass (MS) spectroscopy is now a powerful strategy for large scale profiling of proteins in biological samples, including cell lysates, live cells and in vivo.<sup>1</sup> The combination of chemical protein labeling with MS-based proteome techniques has remarkably facilitated the profiling capability, by defining a specific class of proteins with labeling selectivity.<sup>2</sup> One of the most successful examples represents so-called activity-based protein profiling (ABPP), which was invented by Cravatt's group.<sup>3</sup> Here, only proteins exhibiting an enzymatic activity-of-interest can be labeled with a bio-orthogonal handle. ABPP employs active site-directed chemical reagents (known as activity-based probes: ABPs) to label proteins with a particular enzyme activity in their active pocket, which can focus on the proteome depending on a particular functional state of enzymes, prior to MS-fingerprinting analysis.

In addition to activity, protein localization in a variety of subcellular compartments of live cells should be crucial for proteomics, because the expression level and localization of proteins in each organelle are dynamically varied in response to

environmental conditions and tightly involved in their biological functions. The spatiotemporal changes of proteomes in organelles are responsible for the healthy state of organelles, cells and the consequent live bodies. For example, mitochondria, an energy generating organelle, plays crucial roles in regulating redox states of whole cells and mitochondrial dysfunction induced by a perturbed proteome is associated closely with serious diseases,<sup>4</sup> such as cancer, Alzheimer's and Parkinson's diseases. Therefore, it is crucial to explore what proteins are expressed within a specific organelle and how the proteome changes dynamically with a particular stimulus, thereby addressing a number of fundamental questions that should facilitate medical applications.

In conventional organelle-focused proteomics, subcellular fractionation followed by a high-resolution 2D-gel and/or LC–MS/MS is a widely accepted approach to characterize organelle proteome.<sup>5</sup> However, despite careful preparation, the isolated organelle of interest often suffers from contamination of other

Received: March 1, 2016

Published: May 26, 2016

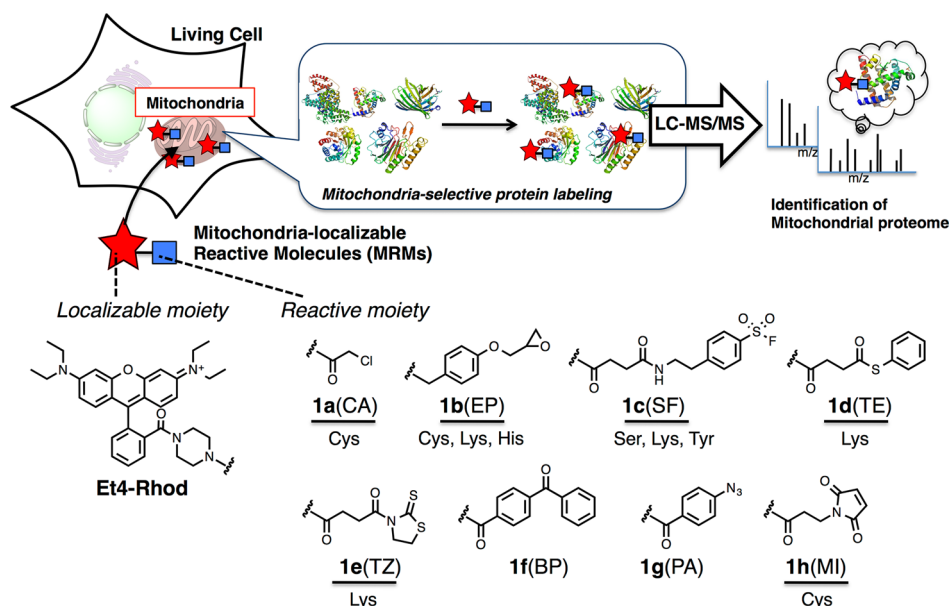


**Figure 1.** Schematic illustration of mitochondria selective protein labeling and profiling by a set of mitochondria-localizable reactive molecules (MRMs). Et4-Rhod, tetraethyl-rhodamine; CA, chloroacetyl; EP, epoxide; SF, sulfonyl fluoride; TE, thiophenyl ester; TZ, thiazolidinethione; BP, benzophenone; PA, phenylazide; MI, maleimide.

organelles and/or potential loss of significant components, which leads to the false-positive and false-negative results. A new method that allows the organelle-focused proteomic mapping without relying on any fractionation was developed recently by Ting and co-workers.<sup>6</sup> They selectively overexpressed an organelle-targeting engineered peroxidase enzyme in mitochondria, by which spatially limited oxidation reactions were facilitated to selectively modify mitochondrial proteins with a biotin affinity tag, followed by extensive MS analysis. Although promising, this enzymatic method always requires expression of an engineered peroxidase. Hence it is difficult to apply the technique to cells or tissues<sup>7</sup> (such as primary neurons and brain slices) that are not readily amenable to exogenous gene expression.<sup>8</sup> In addition, this method uses rather harsh reaction conditions (a high concentration of H<sub>2</sub>O<sub>2</sub>), which may detrimentally perturb natural biological environments<sup>9</sup> and such phenoxy radical-mediated labeling may be unsuited for proteins that lack accessible electron-rich residues such as tyrosine on their surface.<sup>6</sup> To sidestep these drawbacks, chemistry-based proteomics focusing on an organelle would be attractive. Recently, a few of organelle-directed ABPs have been reported, in which organelle-targeting moieties are conjugated with ABPs.<sup>10</sup> However, the ABPs that label a limited enzyme family may not well cover broad-range of proteomes in a target-organelle. For the comprehensive organelle-proteomics, novel approaches not relying on a particular enzyme activity should be required. Toward this end, we recently reported nuclear-localizable reactive molecules (NRMs) containing a DNA-binding motif and a reactive chloroacetyl group.<sup>11</sup> The reagents spontaneously accumulated in the nucleus and selectively reacted with nuclear proteins under intact cell conditions, which allowed the characterization of a range of nuclear proteins by combination with LC-MS/MS analysis.

We describe herein a novel chemical tool for mitochondria-focused proteomics that exploits a set of mitochondria-localizable reactive molecules (MRMs) exhibiting a variety of chemical reactivity and selectivity for endogenous proteins.

Spontaneous concentration and the resultant high concentration of MRMs in mitochondria allowed for spatially restricted chemical reactions with natural mitochondrial proteins of live cells. By combination of this mitochondria-selective labeling with MS-based protein identification, many labeled peptides can be identified. Thus, the chemo-selectivity of these reactive moieties toward a broad array of side chains of endogenous proteins in live cells can be addressed in detail. Owing to its mild labeling conditions and simple protocol, which need neither genetic manipulation nor organelle fractionation, we succeeded in profiling many mitochondrial proteins in live primary cultured neurons and even in brain slices, as well as HeLa cell lines. Furthermore, coupling of this method with a standard quantitative MS technique (SILAC: stable isotope labeling by amino acids in cell culture) enabled to analyze the dynamic change of mitochondrial proteome induced by an oxidative stress.

## RESULTS AND DISCUSSION

**Strategy and Molecular Designs of Mitochondria-Localizable Reactive Molecules (MRMs).** For analyzing the mitochondrial proteome, a set of chemically reactive small molecules equipped with mitochondria-targetable function were designed (Figure 1). Since there are various nucleophilic amino acid residues exposed on the surface of proteins, many electrophilic molecules can potentially react to modify proteins.<sup>12,17</sup> Therefore, it was expected that chemical labeling of proteins located in mitochondria should be facilitated by colocalization of MRMs with mitochondrial proteins, when these are efficiently condensed together in the same small spaces like the case of NRMs.<sup>11</sup> Proteins modified by such spatially limited reactions are then analyzed and identified after cell lysis to collect data on their localization in live cells. That is, MRMs-based labeling allows the transfer of dynamically altered information on mitochondrial proteome in live cells to a permanent covalent bond.

We prepared MRMs composed of both a mitochondria-localizing moiety and a chemically reactive moiety. Tetraethyl-

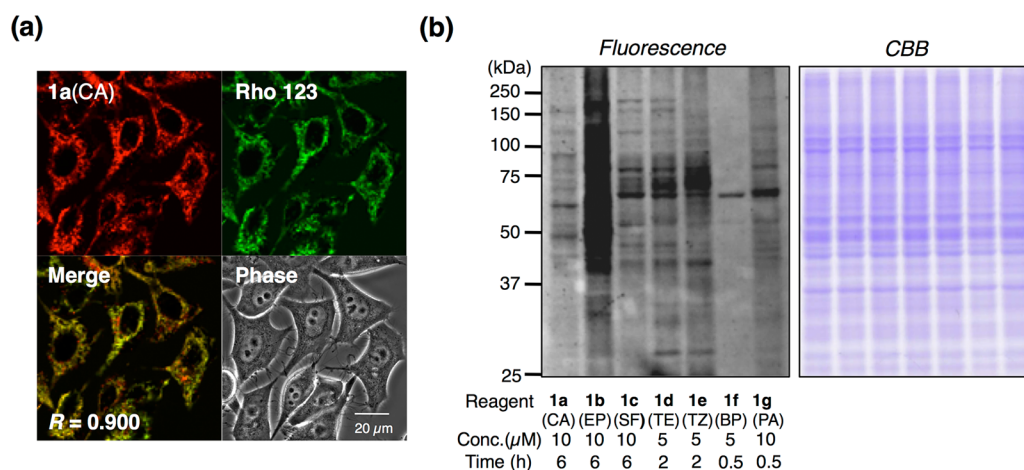


**Figure 2.** Mitochondrial proteome labeling in HeLa cells with MRMs. (a) Confocal micrograph images of HeLa cells stained with **1a(CA)** ( $1.0 \mu\text{M}$ ) and Rhodamine 123 ( $200 \text{ nM}$ ). Colocalization was quantified using Pearson's correlation coefficient ( $R$ ). (b) SDS-PAGE analysis by *in-gel* fluorescence imaging and Coomassie Brilliant Blue (CBB) staining. Reaction conditions: HeLa cells were incubated with MRMs ( $5.0\text{--}10 \mu\text{M}$ ) in serum-free DMEM at  $37^\circ\text{C}$  for  $0.5\text{--}6 \text{ h}$ . In the case of **1f(BP)** and **1g(PA)**, the cells were then UV irradiated ( $40 \text{ min}$ ) on ice. After labeling, the cells were washed, lysed and analyzed by SDS-PAGE. The optimization of labeling conditions with each MRM in living cells was shown in [Figure S5](#) and [S6](#).

rhodamine (Et4-Rhod) was employed as the localizable moiety for mitochondria<sup>13</sup> so that the localization of the MRMs can be readily evaluated by live-cell fluorescent imaging. As a reactive moiety, on the other hand, a variety of reactive functionalities exhibiting distinct amino acid selectivity were used, with the aim of modifying as many amino acids as possible.<sup>14</sup> We explored eight reactive moieties here. Among them, chloroacetyl (CA) and maleimide (MI) are expected to preferentially react with the thiol group of cysteines.<sup>14a,15</sup> Amino groups such as the  $\alpha$ -amine at the *N*-terminus of proteins and the  $\epsilon$ -amine of lysine side chains are reactive with thiophenyl ester (TE) and thiazolidinethione (TZ), which gives a stable amide bond.<sup>16</sup> Epoxide (EP) is reported to react with various nucleophilic amino acids, such as Cys, Lys and His.<sup>17</sup> Sulfonyl fluoride (SF) was used previously to label active sites of Ser proteases as ABPP probes and was also expected to react with Lys and Tyr residues.<sup>18</sup> To label a wider range of amino acids, photoreactive groups such as phenylazide (PA) and benzophenone (BP), conventional photoaffinity labeling reagents, were also employed.<sup>19</sup> [Figure 1](#) summarizes a set of such MRMs and their (expected) amino acid preferences. Synthesis and characterization of the derivatives by NMR and MS spectroscopy was conducted according to [Scheme S1](#).

**Cell Permeability and Localization of MRMs.** The cell permeability and mitochondrial localization of a set of MRMs in HeLa cells were evaluated initially by confocal laser scanning microscopy (CLSM). Rapid (within  $15 \text{ min}$ ) and spontaneous localization in mitochondria were observed for the majority of these molecules. For example, the CLSM image of HeLa cells treated with **1a(CA)** for  $15 \text{ min}$  is shown in [Figure 2a](#). This merged well with the image stained by Rhodamine123, a representative mitochondrial localization marker.<sup>20</sup> Other MRMs such as **1b(EP)**, **1c(SF)**, **1d(TE)**, **1e(TZ)**, **1f(BP)** and **1g(PA)** gave almost identical CLSM images to the one observed with **1a(CA)** ([Supplementary Figure S1](#)). The excellent overlap and the resultant high Pearson's correlation coefficient (more than  $0.85$ ) indicated that these MRMs efficiently accumulated in mitochondria of live HeLa cells. Such mitochondrial localization did not occur in HeLa cells pretreated with carbonyl cyanide *m*-chlorophenylhydrazine

(CCCP), a standard uncoupler of the mitochondrial membrane potential<sup>21</sup> ([Figure S2](#)), revealing that spontaneous accumulation of these MRMs was driven by the high membrane potential of mitochondria.

We also spectroscopically determined the intracellular concentration of these MRMs after lysis of the HeLa cells ([Figure S3](#)). In the optimized conditions for the below-mentioned protein labeling experiments, the concentrations of **1a(CA)**–**1g(PA)** are in the range of  $24$  to  $213 \mu\text{M}$  inside the cell. These values correspond to a  $4$  to  $21$ -fold condensation relative to the concentration of the MRMs added extracellularly. Given the volume of mitochondria in live HeLa cells, it is regarded that the condensation effect is further enhanced by  $\sim 3$ -fold,<sup>22</sup> which could facilitate the intermolecular labeling reactions in mitochondria. In contrast, the maleimide-appended Et4-Rhod **1h(MI)** gave the rather weak intracellular fluorescence, indicating its poor cell permeability ([Figure S4](#)). Hence, **1h** was omitted from our set of MRMs.

**Labeling and Identification of Proteins in Mitochondria of HeLa Cells.** Having a set of cell permeable MRMs in hand, we then evaluated their reactivity with natural proteins in HeLa cells by SDS-PAGE analysis. After the addition of each MRM (**1a(CA)**–**1g(PA)**) to the culture medium of HeLa cells, followed by incubation, the cells were lysed and the resultant lysate was subjected to SDS-PAGE. As shown in [Figure 2b](#), the labeled protein bands were detected by fluorescence due to the Et4-Rhod fluorophore, which indicated that the band pattern was distinct and dependent on the labeling reagent. In contrast to the many bands observed for most MRMs, **1f(BP)** gave only a few bands with noticeable band intensity. In addition, the CLSM image after **1a(CA)** treatment was not altered by the addition of CCCP, whereas clear mitochondrial images were not observed in the case of the CCCP-pretreated HeLa cells ([Figures S2](#) and [S7](#)). These data additionally support the covalent attachment of **1a(CA)** to proteins in mitochondria.

Identification of the labeled proteins in detail was subsequently carried out by LC-MS/MS analysis. The Et4-Rhod fluorophore serves as a vehicle for targeting organelles and is also an excellent antigen to elicit antibodies that should enrich labeled proteins and peptides in downstream immuno-

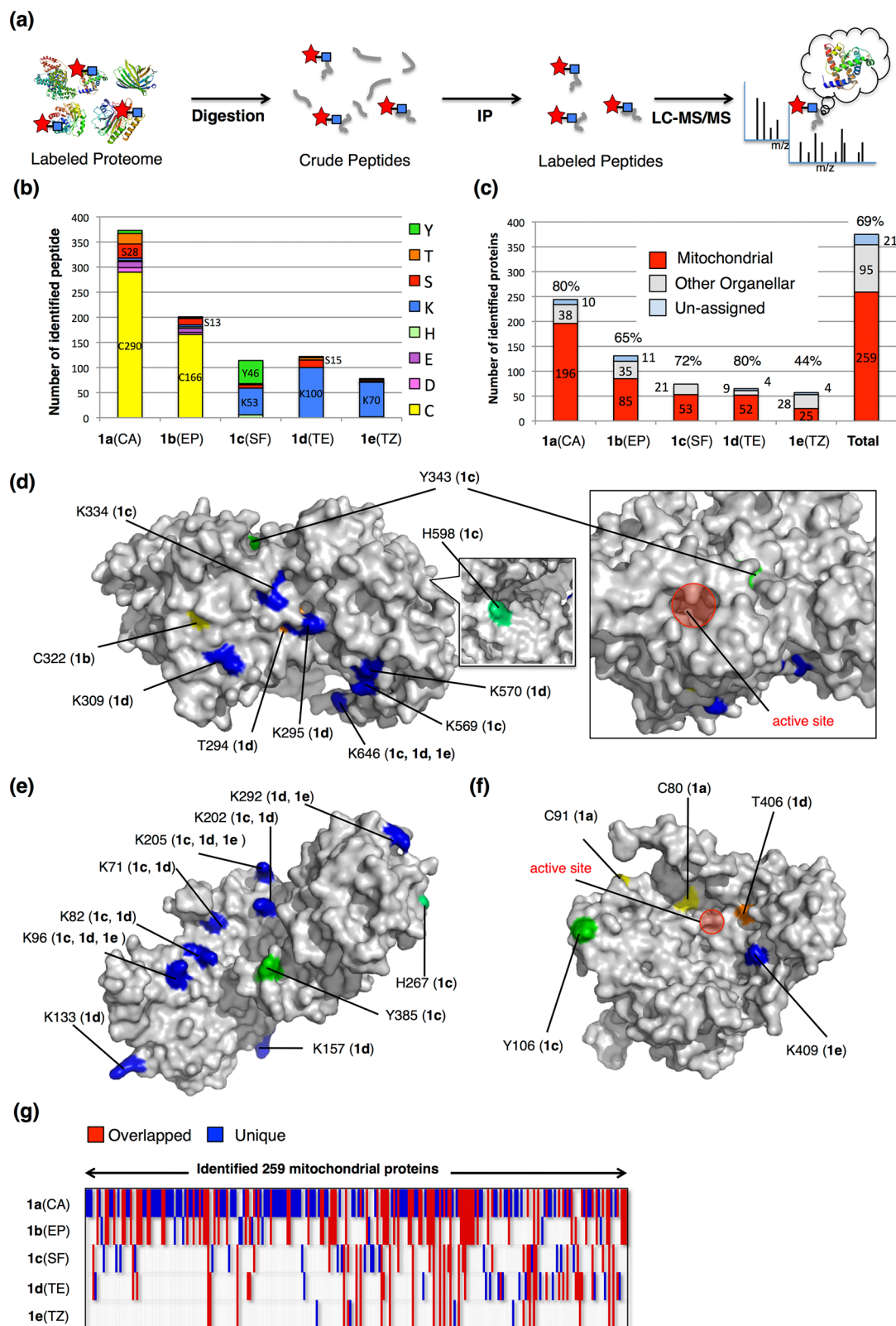


**Figure 3.** Identification and profiling of Et4-Rhod labeled proteins and their modified residues. (a) Workflow of labeled-peptide/protein identification by the gel-free protocol. (b) The number of identified peptides and their labeled residues determined by LC-MS/MS analysis. Y, tyrosine; T, threonine; S, serine; K, lysine; H, histidine; E, glutamic acid; D, aspartic acid; C, cysteine. (c) The number of proteins identified by LC-MS/MS analysis from HeLa cells and the ratio of mitochondrial proteins. The identified proteins were classified by cellular location using the protein ontology information provided in the UniProt database. (d, e, f) 3D structures of (d) HADHA, (e) HSPD1 and (f) SHMT2 with labeled residues (colored). These protein models from SWISS-MODEL were manipulated and rendered in PyMOL. Additional images of these proteins from different viewpoints and other representative proteins are shown in Figure S9 and S10. (g) Color map representation of identified mitochondrial proteins

Figure 3. continued

proteins. Proteins that were uniquely or overlappingly identified by each MRM are highlighted in blue or red, respectively. Detailed information on identified proteins is presented in [Supplementary Data S1](#).

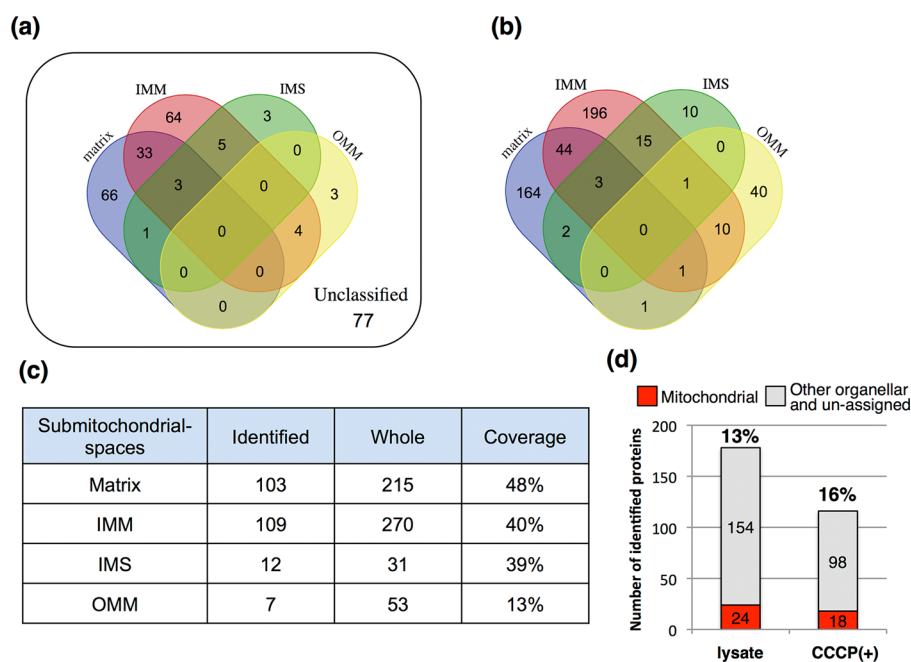


**Figure 4.** Submitochondrial localization of identified proteins and reaction specificity of MRMs. (a) Venn diagram representing the submitochondrial localization of identified proteins from HeLa cells. On the basis of the GO terms, proteins identified as mitochondrial proteins were further classified into “matrix”, “inner membrane (IMM)”, “intermembrane space (IMS)” and “outer membrane (OMM)”. It should be noted that some proteins are classified into plural submitochondrial regions. The list of identified proteins with their submitochondrial localization can be found in [Supplementary Data S1](#). (b) Venn diagram of submitochondrial localization of whole mitochondrial proteins with prior submitochondrial localization data in MitoCarta<sup>31</sup> or Uniprot database. (c) Coverage of identified proteins in each submitochondrial space. Identified, the number of identified proteins; Whole, the number of mitochondrial proteins registered in the databases. (d) The number of identified proteins and the ratio of mitochondrial proteins in negative control experiments. HeLa cell lysate and CCCP-pretreated HeLa cells were incubated with 1a(CA), followed by LC-MS/MS analysis.

precipitation (IP) assays. We thus prepared an anti-Et4-Rhod antibody<sup>23</sup> and used this antibody for concentrating the labeled proteins/peptides prior to MS/MS analysis. To directly detect the labeled peptides and to minimize the contamination during IP and gel separation, we exploited the modified “gel-free” method that was originally reported by Cravatt et al. (Figure 3a).<sup>24</sup> In our protocol, the labeled peptides rather than proteins were concentrated by IP, which were then analyzed by LC-MS/MS without SDS-PAGE. In the case of 1a(CA), for example, we detected 373 labeled peptides, thus the labeled amino acids were identified (Figure 3b, Table S1 and [Supplementary Data S1](#)). Clearly, Cys-labeled peptides (290 (78%)) were readily detected as the largest group. The second largest groups were Ser- (8%) and Thr- (6%) labeled peptides, where the amino acid preference is consistent with the intrinsic chemical reactivity of CA. A similar Cys preference was also observed by 1b(EP) with labeling of 83% of the peptides and Ser-labeled peptides were the second largest group (6%). On the other hand, 1d(TE) gave 82% of Lys-labeled peptides and Ser-labeled peptides (12%) formed the second largest group. This preference was almost the same as that of 1e(TZ) (90% for Lys). In the case of 1c(SF), it was characteristic that Lys (46%) and Tyr (40%) were the two predominant amino acids labeled. Peptides labeled by 1f(BP) and 1g(PA) were not detected, which may be due to the instability of the formed covalent bond and/or the formation of unexpected adducts. Of

note, identifying labeled peptides (not proteins) that we conducted here enabled us to address the amino acid preference of these reactive moieties in live cells explicitly, which revealed that the chemical selectivity in live cells roughly reflected those expected in conventional organic reactions. Additionally, this strongly indicated that most of the detected labeled peptides did not come from artifacts of the present MS fingerprinting protocol.

The data derived from these labeled peptide sequences were used to identify the labeled proteins. Figure 3c and Table S2 summarizes the identified proteins and their localization. The use of 1a(CA) labeled 244 proteins, and 196 of these proteins are assigned as mitochondrial proteins (80%). Similarly, 85 (among 131), 53 (among 74), 52 (among 65) and 25 (among 57) mitochondrial proteins were identified by 1b(EP), 1c(SF), 1d(TE) and 1e(TZ), respectively. Figure 3d and Figure S9 show a representative protein, trifunctional enzyme subunit alpha, mitochondrial (HADHA), identified by 15 labeled peptides, where 12 sites were modified with 5 MRMs. Similarly, 18 sites of 60 kDa heat shock protein, mitochondrial (HSPD1) and 7 sites of Serine hydroxymethyltransferase, mitochondrial (SHMT2) were labeled with 5 and 4 MRMs, respectively (Figure 3e, 3f and Figure S9). These results clearly showed that different labeling reagents reacted with distinct peptide sequences and/or amino acids (despite partial overlap) and more importantly these labeled residues were mainly exposed

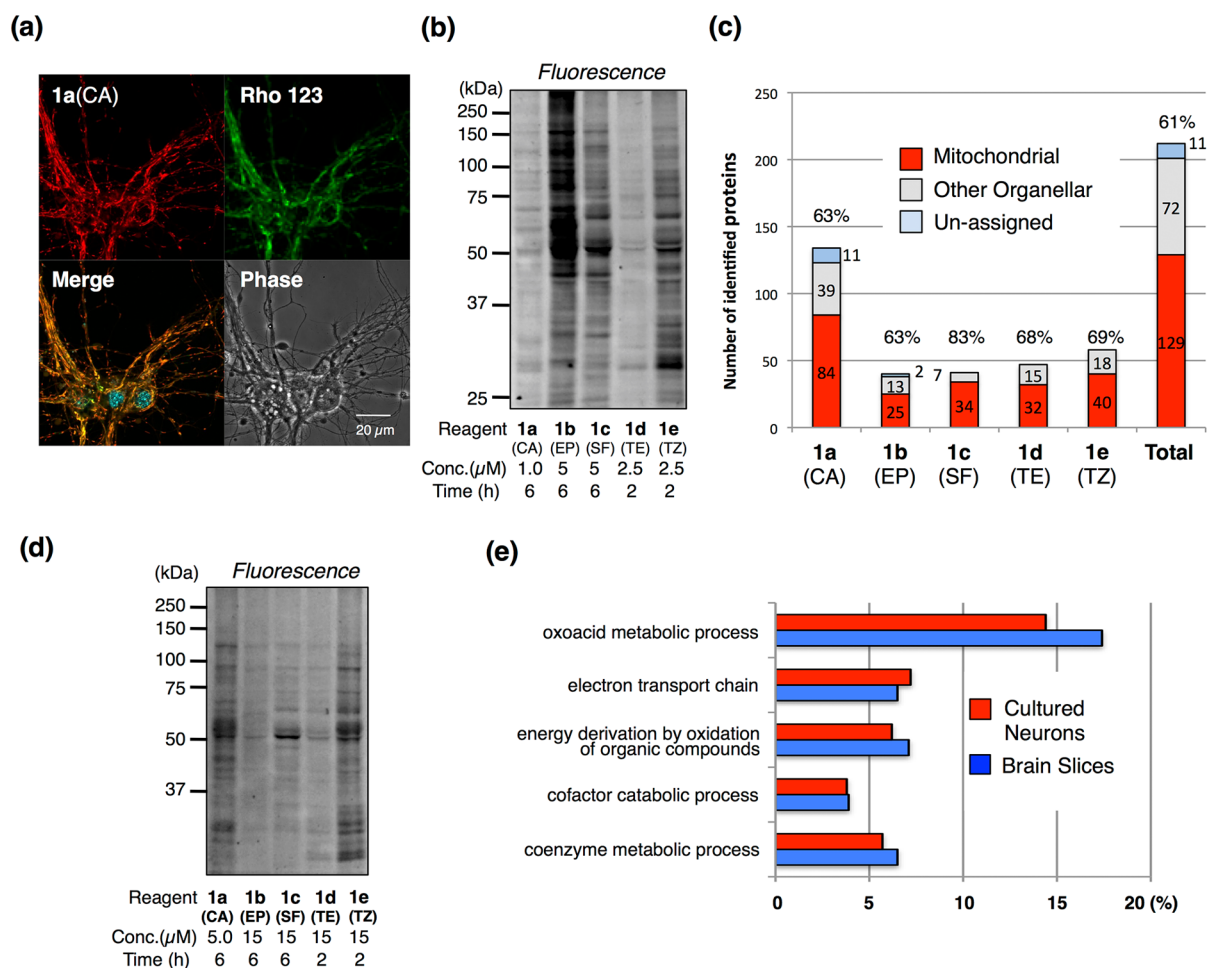


**Figure 5.** Mitochondrial proteome labeling in primary cortical neurons and brain slices with MRMs. (a) Confocal micrograph images of neurons stained with 1a(CA) (1.0  $\mu\text{M}$ ), Rhodamine 123 (200 nM) and Hoechst 33342 (1.0  $\mu\text{M}$ ). (b) SDS-PAGE analysis by *in-gel* fluorescence imaging. Reaction conditions: primary cortical neurons  $6 \times 10^5$  cells (16-d-old Sprague–Dawley rat embryos) were incubated with MRMs (1.0–5.0  $\mu\text{M}$ ) in serum-free DMEM at 37  $^\circ\text{C}$  for 2–6 h. After labeling, the cells were washed, lysed and analyzed by SDS-PAGE. (c) The number of proteins identified by LC–MS/MS analysis from primary cultured neurons and the ratio of mitochondrial proteins. (d) SDS-PAGE analysis by *in-gel* fluorescence imaging. Reaction conditions: Brain (cerebrum) slices (250  $\mu\text{m}$  thickness) prepared from P14–21 ICR mice were incubated with MRMs (5.0–15  $\mu\text{M}$ ) in the ACSF solution at room temperature for 2–6 h under 95%  $\text{O}_2$ /5%  $\text{CO}_2$ . After labeling, the tissues were washed, lysed and analyzed by SDS-PAGE. (e) Functional classification of identified proteins from primary cultured neurons and brain slices by LC–MS/MS analysis (enrichment *P*-value by DAVID < 0.0002).

on the protein surface and not buried in the active pocket. Such surface labeling was observed in most of identified proteins whose 3D-structures were available or postulated<sup>25</sup> (Figure S9 and S10), suggesting the mitochondria-localized labeling was facilitated by simple intermolecular reactions in limited spaces,<sup>26</sup> and not by specific activity/affinity with proteins (Figure S12). It is also evident that the number and sort of identified proteins were largely dependent on the reactive moiety of the MRMs. More importantly, each MRM can label unique proteins, while some overlap with each other. That is, Figure 3g and Table S3 show that 105 mitochondrial proteins were uniquely identified by 1a(CA), and 10 by 1b(EP), 18 by 1c(SF), 14 by 1d(TE), and 4 by 1e(TZ). These results clearly highlight the advantage of using a variety of chemically reactive moieties to cover a wide range of proteomes in mitochondria.

The annotation analysis of the whole labeled proteins revealed that 69% are assigned to mitochondria-localizing proteins, 6% of the proteins were not assigned (unassigned) to a location and 25% were assigned as nonmitochondrial proteins (Figure 3c). The identified mitochondrial proteins were further

classified into submitochondrial localizations, namely, “matrix”, “inner membrane (IMM)”, “intermembrane space (IMS)” and “outer membrane (OMM)” (Figure 4a). Among 259 mitochondrial proteins identified in our study, 182 proteins can be annotated by submitochondrial localization on the basis of the Gene Ontology (GO) terms. We found that 163 proteins (66 + 33 + 64) were assigned to the matrix or IMM but not IMS or OMM localization, while 19 proteins were assigned to the IMS or OMM localization. That is, our MRM mainly labeled proteins localized in matrix or IMM of mitochondria. Moreover, it was revealed that the coverage of OMM proteins, defined by the percentage of identified OMM proteins over the whole OMM proteins, is lower (13%) than that of matrix (48%), IMM (40%) and IMS (39%) (Figure 4b and 4c). These results clearly show our MRMs mainly react with proteins inside mitochondria, which is consistent with the assumed submitochondrial localization of Et4-Rhod.<sup>27</sup> Among the unassigned proteins, there are some proteins shuttling between mitochondria and ER (or other organelles), such as Reticulon-4<sup>28</sup> and Apolipoprotein C-III,<sup>29</sup> which may be reassigned as

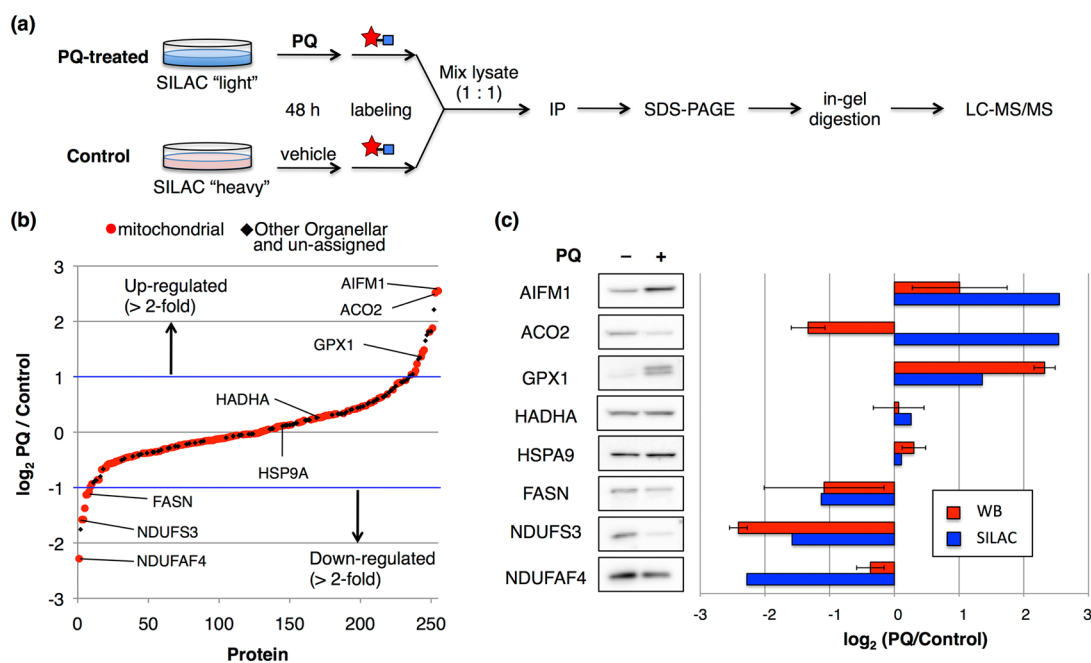


**Figure 6.** Quantitative MS analysis of the change of mitochondrial proteome under an oxidative stress. (a) Schematic illustration of SILAC experiments coupled with MRMs to quantify mitochondrial proteome changes in paraquat (PQ)-treated HeLa cells. PQ-treated cells grown in the light SILAC medium and nontreated cells grown in the heavy SILAC medium (control) were labeled with **1a**(CA) and lysed. Protein extracts from the light and heavy cells were mixed in a 1:1 ratio, and then the Et4-Rhod-labeled proteins were enriched by IP using anti-Et4-Rhod antibody, followed by in-gel tryptic digestion and LC-MS/MS analysis. (b) Log<sub>2</sub> ratio plot (PQ-treated (light) cells/control (heavy)) of identified proteins. Proteins assigned as mitochondrial are colored in red in the plot. Proteins without mitochondrial annotation are colored in black. (c) Western blotting analysis of PQ-induced changes in expression levels of the selected proteins ( $n = 3$  ( $\pm$  standard deviation)) and their comparison with data from SILAC.

mitochondria-localized ones. The 25% nonmitochondrial proteins detected offers some caution to this method providing false positive information on protein localization. This is plausibly due to side reactions with highly abundant proteins such as cytoskeletal proteins,<sup>30</sup> the misdistribution of the MRMs during the labeling process and mischaracterization of the labeled peptides during LC-MS/MS analysis. However, as mentioned above, these MRMs were efficiently concentrated in mitochondria of live HeLa cells. Additionally, negative control experiments using the HeLa lysate and CCCP-pretreated HeLa cells as the labeling sample (**1a**(CA)) confirmed that the content of the mitochondria-localizing proteins decreased to only 13 and 16%, respectively (Figure 4d, Figure S13 and Supplementary Data S5). Given these results, it is concluded that most of MRMs mainly react with mitochondrial proteins by spontaneous condensation in the mitochondrial limited space under live cell conditions and therefore MRMs are suitable tools for mitochondria-selective chemical proteomics.

**Application of MRMs to Primary Cultured Neurons and Brain Slices.** Our MRMs-based chemical proteomics method requires neither pretreatment of cells such as gene transfection, nor careful (and time-consuming) organelle fractionation processes. Thus, this method can be applied to mitochondria-focused proteomics of primary cells and/or more complicated natural samples such as brain tissue. As a representative example, we explored the mitochondrial proteome of primary cultured neurons. Each of the five MRMs were mixed with cultured neural cells isolated from the cerebral cortex of the rat brain, followed by incubation. The localization of each MRM was confirmed by CLSM imaging (Figure 5a and Figure S14), showing that the MRMs spontaneously accumulated to mitochondria of the rat neuron.

Using a similar protocol employed for the HeLa cells, SDS-PAGE analysis and gel-free protein identification were conducted (Figures 5b, 5c and Supplementary Data S2). Interestingly, the amino acid preference of each MRM determined by the labeled peptides was almost identical with the experimental data obtained from HeLa cells (Table S4). Additionally, we identified 212 proteins that included at least 129 (~61%) mitochondrial proteins using 5 MRMs (Figure 5c and Table S5).

Moreover, the mitochondrial proteomics of brain slices was accomplished by mixing each MRM with acutely prepared brain slices of mice cerebral cortexes. As shown in Figure 5d, labeled protein bands were observed in all MRMs, while the band intensity of **1b**(EP) was quite weak when compared with the labeling in primary neurons. This is probably due to **1b**(EP) poor tissue permeability. One hundred proteins were assigned as mitochondrial proteins from this brain slice experiments, which corresponded to 64% of the total number of proteins identified (Figure S15, Table S6 and Supplementary Data S3). This ratio and amino acid preference are in agreement with those of HeLa cells and primary cultured neurons (Table S7). We subsequently classified these proteins on the basis of their function using DAVID bioinformatics resources (Figure 5e).<sup>32</sup> It was revealed that the majority of the proteins labeled in the brain slices are involved with unique mitochondrial functions, such as oxoacid metabolic process, electron transport chain and energy derivation by oxidation of organic compounds. This labeling pattern is functionally identical with that obtained in labeling the primary neurons with the MRMs. Although the coverage of mitochondrial proteins are not sufficiently high likely due to the low tissue-permeability of MRMs, our MRM-based method clearly has valuable features: (i) simplicity of the

experimental protocol; (ii) minimization of unfavorable effects to live samples; and (iii) successful chemical proteomics of mitochondria for sensitive and complicated biological samples that are not easily amenable to exogenous gene manipulation.<sup>8</sup>

**Chemical Profiling of a Dynamic Proteome during an Oxidant-Induced Apoptosis Process.** We finally applied this MRM approach to explore the dynamics of mitochondrial proteome of live cells in response to a cellular stress. As a proof-of-principle, we combined our MRM-based method with SILAC, a quantitative MS analysis technique,<sup>33</sup> in order to investigate the change of mitochondrial proteome of HeLa cells during an apoptosis process induced by paraquat (PQ),<sup>34</sup> an oxidative stress inducer. HeLa cells grown in light SILAC media were incubated with PQ for 48 h, followed by 1a(CA) (5.0  $\mu$ M, 6 h), whereas cells grown in heavy SILAC media were only treated with 1a(CA) in the absence of PQ (Figure 6a). The PQ-induced apoptosis was validated by a cleavage of PARP-1, a standard marker of apoptosis (Figure S16). It was also confirmed that 1a(CA) localized in mitochondria of the apoptotic HeLa cells like as normal cells (Figure S17) and the intracellular concentration did not substantially change by PQ treatment (Figure S18). As shown in Figure S19, the fluorescent band patterns of SDS-PAGE gel were well identical between the PQ-treated and PQ-nontreated cells, indicating the PQ-treatment did not largely impact most of mitochondrial proteins of HeLa cells. To obtain the optimal performance for quantitative MS analysis, we carried out a standard protein identification protocol including IP of the labeled proteins (not peptides), followed by MS fingerprinting analysis. 255 proteins were identified and quantified in total from three independent biological replicates (Figure S20), among which 166 proteins (65%) were classified into mitochondrial proteins, showing that our MRM-based labeling works well in apoptotic cells (Figure 6b and Supplementary Data S4). Of the quantified proteins, 21 proteins were up-regulated by more than 2-fold in PQ-treated HeLa cells (Table S8), which included “glutathione peroxidase 1 (GPX1)”, “Peroxiredoxin-1 (PRDX1)” and “Peroxiredoxin-2 (PRDX2)” that have been reported to increase under oxidative stress or apoptotic processes.<sup>35</sup> Functional annotation analysis of the 21 up-regulated proteins using DAVID revealed that terms of apoptosis-related biological process mediated by reactive oxygen species (ROS), such as “regulation of apoptosis” (36%,  $p$  value:  $1.54 \times 10^{-3}$ ), “regulation of programmed cell death” (36%,  $p$  value:  $1.54 \times 10^{-3}$ ), “response to hydrogen peroxide” (18%,  $p$  value:  $6.41 \times 10^{-3}$ ), “cellular response to reactive oxygen species” (18%,  $p$  value:  $1.21 \times 10^{-2}$ ), and “positive regulation of programmed cell death” (23%,  $p$  value:  $1.25 \times 10^{-2}$ ), were significantly enriched (Figure S21). It was also found that 7 mitochondrial proteins were down-regulated by more than 2-fold (Table S9), among which 3 proteins (NDUFS3, NDUFS1 and FASN) are previously reported to decrease under oxidative stress or apoptotic processes.<sup>36</sup> These data obtained by MRM-based SILAC technique consistently reflect the dynamic change of mitochondrial proteome of HeLa cells in response to the oxidative stress.

In order to further evaluate our quantitative MS data, Western blotting (WB) analysis was carried out. We selected 6 representative mitochondrial proteins from the list of identified proteins with substantial (>2-fold) changes in the SILAC experiment. These include three up-regulated proteins (AIFM1, ACO2, GPX1) and three down-regulated proteins (NDUFAF4, NDUFS3, FASN). Among them, three proteins (AIFM1,

ACO2, NDUFAF4) are previously unknown to change in the expression levels through apoptosis, whereas substantial change of the expression level for the other three (GPX1, NDUFS3, FASN) are already reported. Besides, two proteins (HADHA, HSPA9) showing not substantial alterations in the SILAC ratios were also evaluated by WB analysis. As shown in Figure 6c, WB data for seven proteins, AIFM1, GPX1, NDUFAF4, NDUFS3, FASN, HADHA and HSPA9 indicated the same tendencies in the change of the expression levels as that determined by the SILAC experiment. These results clearly validated the data of our quantitative MS analysis exploiting MRM-based labeling strategy. Notably, both up-regulation of AIFM1 and down-regulation of NDUFAF4 in the ROS-mediated apoptosis process are identified for the first time, to the best of our knowledge. AIFM1, apoptosis-inducing factor 1, is an NADH oxidase and implicated in a caspase-independent pathway of programmed cell death.<sup>37</sup> NDUFAF4, NADH dehydrogenase [ubiquinone] 1 alpha subcomplex assembly factor 4 which is involved in the assembly of respiratory chain complex I, is reported to negatively regulates apoptosis.<sup>38</sup> Importantly, these proteins are supposed to be associated with some of mitochondrial diseases,<sup>39</sup> such as neuropathy and Parkinson disease. Thus, the present new finding may encourage us to facilitate a more detailed study on biological roles of these proteins in dysfunctional mitochondria.

On the other hand, WB data of ACO2, mitochondrial aconitate hydratase, did not agree with that of the SILAC experiment. To examine this discrepancy, we focused on the labeling sites of ACO2. MS analysis successfully identified Cys385 and Cys451 as the labeling sites, both of which are involved in binding to an iron–sulfur [4Fe-4S] cluster, an active site of ACO2. It is also reported that this [4Fe-4S] cluster is destructed and removed by ROS,<sup>40</sup> leading to a conformational change of ACO2 and its subsequent degradation. Given these reports, it is reasonably considered that the removal of [4Fe-4S] cluster from ACO2 by PQ-induced ROS enhances the accessibility (i.e., reactivity) of the Cys385 and Cys451 with MRMs, resulting in an increase of the SILAC ratio despite of a decline of ACO2 expression level. While this example may point out a false positive case of our MRM-based SILAC approach, it also suggests that the careful examination of our data could give us interesting information on the structure and/or activities changes of a mitochondrial protein in living cells.

Overall, these experiments undoubtedly demonstrate that our MRM-based method provides a convenient and quantitative approach to efficiently focus on representative proteins in the dynamic change of mitochondrial proteins, in combination with a standard quantitative proteomic technique.

## CONCLUSIONS

We have developed a set of MRMs as novel chemical reagents for organelle-focused proteomics. This gave us a remarkably simple experimental protocol of organelle-selective labeling that is compatible with conventional LC–MS/MS and MS-fingerprinting techniques. This method explicitly addressed the chemical reactivity and selectivity of various reactive groups in live cells and identified the mitochondrial proteome in essentially natural biological habitats, including live primary cultured neurons, brain slices and HeLa cells. Quantitative profiling and characterizing particular proteins have also been accomplished using this method, whose expression levels were



found to change dynamically during an oxidant-induced apoptosis.

The present MRM-based method was able to label and identify a relatively small fraction of the mitochondrial whole proteome that is roughly estimated to contain 1000–1500 proteins.<sup>4,41</sup> The limited coverage may be partially attributed to the biased submitochondrial distribution of the Et4-Rhod-based MRMs (in the matrix and inner membrane). This issue would be overcome by varying the localizable moiety to target different areas within the mitochondria.<sup>42</sup> Moreover, given the modular structures of MRMs, a rational extension of this strategy targets other organelles by varying the localizable moiety to cover a whole proteome in live cells and tissues. We envision that the sets of organelle-localizable reactive molecules can be widely used against a variety of intact cells involved in organelle-relevant diseases to identify molecular details by profiling differentiating proteomes at high resolution.

## ■ EXPERIMENTAL SECTION

**Synthesis.** All synthetic procedures and compound characterizations are described in the [Supporting Information](#).

**General Materials and Methods for the Biochemical/Biological Experiments.** Unless otherwise noted, all proteins/enzymes and reagents were obtained from commercial suppliers (Sigma-Aldrich, Tokyo Chemical Industry (TCI), Wako Pure Chemical Industries, Sasaki Chemical, Bio-Rad, or Watanabe Chemical Industries) and used without further purification. UV–vis absorption spectra were acquired on a Shimadzu UV-2550 spectrophotometer. SDS-polyacrylamide gel electrophoresis (SDS-PAGE) and Western blotting were carried out using a Bio-Rad Mini-Protean III electrophoresis apparatus. Fluorescence gel images and chemical luminescent signals using Chemi-Lumi one (Nacalai Tesque) or ECL Prime (GE Healthcare) were acquired with an imagequant LAS4000 (GE Healthcare). Cell imaging was performed with a confocal laser scanning microscope (CLSM, Olympus, FV10i) using 60× objectives, and images were analyzed using accompanying FV10i-ASW 3.0 Viewer software.

**CLSM Analysis of HeLa Cells.** HeLa cells ( $2.0 \times 10^5$  cells) were cultured on 35 mm glass based dishes in Dulbecco's Modified Eagle Medium (DMEM) supplemented with 10% fetal bovine serum (FBS) and 1% Antibiotic-Antimycotic (Anti-Anti, gibco) under a humidified atmosphere of 5% CO<sub>2</sub> in air at 37 °C for 24 h. The cells were washed twice with serum-free DMEM (HEPES modified, no Phenol Red), and incubated in serum-free DMEM containing MRMs (1.0 μM) for 15 min. The intracellular localization of these reagents was analyzed by CLSM. As a negative control, HeLa cells were preincubated with CCCP (5.0 μM) for 5 min before addition of MRMs.

**Mitochondrial Proteome Labeling with MRMs in HeLa Cells.** HeLa cells ( $1.0 \times 10^6$  cells) were cultured on 10 cm dishes under a humidified atmosphere of 5% CO<sub>2</sub> in air at 37 °C for 48 h in DMEM. The cells were washed twice with serum-free DMEM, and incubated in serum free DMEM containing MRM (5–10 μM) for 0.5–6 h. In the case of using photoreactive probes, such as **1f**(BP) and **1g**(PA), the cells were washed twice with chilled PBS, and then exposed to 365 nm light with a handy UV lamp (4 W) at 1 cm distance from the top of cell culture dish for 40 min on ice. After labeling reaction, the cells were washed twice with chilled PBS, lysed by sonication in modified-RIPA buffer (25 mM Tris, 150 mM NaCl, 1% Sodium dodecyl sulfate, 1% Nonidet P-40, 1% sodium deoxycholate, pH 7.6) containing 1% protease inhibitor cocktail set III (Novagen) at 4 °C. Proteins were precipitated with chilled acetone, and the pellets were solubilized by sonication in modified-RIPA buffer. The solubilized proteins were normalized for protein concentration (BCA assay kit, Thermo) to 1.0 mg/mL, and then mixed with 1/4 volume of 5 × SDS–PAGE loading buffer (pH 6.8, 325 mM Tris, 20% sucrose, 15% SDS, 0.03% bromophenol blue) containing 250 mM DTT and vortexed for 30 min. The samples were resolved by SDS-PAGE (8.0 μg protein/lane),

and the Et4-Rhod labeled proteins were visualized fluorescence gel imager (LAS4000, GE Healthcare).

**Preparation of LC–MS Samples (In-Solution Digested Samples).** After mitochondrial proteome labeling with MRMs, the cells were lysed with RIPA buffer (25 mM Tris, 150 mM NaCl, 0.1% Sodium dodecyl sulfate, 1% Nonidet P-40, 1% sodium deoxycholate, pH 7.6). All proteins were precipitated with chilled acetone, and solubilized by sonication in modified-RIPA buffer. Protein concentration was determined by BCA assay and normalized to 2.0 mg/mL (total volume 1 mL). The samples were diluted into 1 mL of 12 M urea (final conc. 6 M), reduced with 20 mM DTT at 65 °C for 5 min, and alkylated with 40 mM iodoacetamide at 37 °C for 30 min. After precipitation with 20% methanol containing acetone (8 mL), 500 μg of proteins were treated with following two methods (method A or B).

In method A, the pellet of proteins was solubilized by sonication in 500 μL of sodium deoxycholate (SDC) buffer (0.1% SDC, 1 M urea, 10 mM ammonium bicarbonate), and digested with 5 μg of trypsin (Thermo, MS grade) overnight at 37 °C. The mixture was boiled at 65 °C for 5 min to inactivate trypsin. To remove the surfactant, phase-transfer surfactant protocols were conducted.<sup>24</sup> Briefly, the digested solution was mixed with 500 μL of ethyl acetate, acidified with 2.5 μL of TFA, and shaken for 1 min. The mixture was centrifuged at 16 000g for 2 min, and the organic phase was removed. The aqueous phase was washed with 500 μL of ethyl acetate again, and neutralized with 200 mM Tris-HCl (pH 7.4).

In method B, 500 μg of proteins were solubilized by sonication in 250 μL of urea buffer (4 M urea, 100 mM Tris-HCl, pH 8.0). The solution was diluted with 250 μL of 100 mM Tris-HCl (pH 8.0), and incubated with 5 μg of trypsin overnight at 37 °C. The mixture was boiled at 65 °C for 5 min and diluted with 1.5 mL of Tris-HCl (pH 8.0).

The resulting solutions in method A and B were incubated with 5.0 μL of anti-Et4-Rhod antiserum for 6 h at 4 °C with continuous rotation, followed by addition of 50 μL of nProtein A sepharose 4 Fast Flow (GE Healthcare, 50% slurry in PBS) and further rotation at 4 °C for 2 h. The beads were washed 5 times with PBS (1 mL) and water (1 mL). The peptides labeled with Et4-Rhod were eluted with 40 μL of 50% water/CH<sub>3</sub>CN (0.1% TFA) × 2 and 40 μL of CH<sub>3</sub>CN (0.1% TFA) × 2. These eluents were collected and centrifuged (12 000g, 5 min). The supernatant was freeze-dried, redissolved with 20 μL of 2% CH<sub>3</sub>CN/water containing 0.1% TFA, and further centrifuged at 16 000g for 5 min. This supernatant (2–4 μL) was subjected to LC–MS analysis. The list of identified proteins obtained by method A and B were integrated into an output file. Protein identification experiments using HeLa cells and primary cortical neuronal culture were independently performed twice.

**Preparation of LC–MS Samples (SILAC Samples).** HeLa cells were grown in “heavy” SILAC media (DMEM, Thermo) containing 100 μg/mL of <sup>13</sup>C<sub>6</sub>, <sup>15</sup>N<sub>2</sub>-Lys (Cambridge Isotope Laboratories) and <sup>13</sup>C<sub>6</sub>, <sup>15</sup>N<sub>4</sub>-Arg (Cambridge Isotope Laboratories) or “light” SILAC media containing <sup>12</sup>C<sub>6</sub>, <sup>14</sup>N<sub>2</sub>-Lys (Thermo) and <sup>12</sup>C<sub>6</sub>, <sup>14</sup>N<sub>4</sub>-Arg (Thermo) supplemented with 10% dialyzed FBS (Gibco) and 1% Anti-Anti under a humidified atmosphere of 5% CO<sub>2</sub> in air at 37 °C. The cells were passaged at least five times in the SILAC media before being used for analysis. The isotope-labeled cells ( $6.0 \times 10^5$  cells) were seeded on 10 cm dishes and incubated for 24 h in the SILAC media. The “light” labeled cells were incubated with light SILAC media containing Paraquat (PQ) (100 μM) for 48 h, while the “heavy” labeled cells were treated with heavy SILAC media containing vehicle (water). Both the light and heavy cells were washed twice with PBS, and incubated in serum free SILAC media containing **1a**(CA) (5.0 μM) for 6 h. After labeling reaction, the cells were washed twice with chilled PBS, lysed by sonication in modified-RIPA buffer containing 1% protease inhibitor cocktail at 4 °C. Proteins were precipitated with chilled acetone, and the pellets were solubilized by sonication in modified-RIPA buffer. The solubilized proteins were normalized for protein concentration with BCA assay. Equal amounts of protein from heavy (500 μg/250 μL) and light (500 μg/250 μL) samples were mixed in a 1:1 ratio, and the mixture were diluted with PBS into 1.0 mL. The samples were precleared against 100 μL of nProtein A

sepharose 4 Fast flow at 4 °C for 30 min. After centrifugation, the supernatant was collected and incubated with anti-Et4-Rhod (10.0 μL) at 4 °C overnight with continuous rotation, followed by addition of 100 μL of nProtein A sepharose 4 Fast flow. After incubation at 4 °C for 2 h, the beads were washed 5 times with RIPA buffer (1.0 mL), and then boiled in 2× SDS-PAGE sample buffer (25 μL) containing 100 mM DTT for 3 min. The supernatant (15 μL) was loaded to SDS-PAGE. The samples were resolved 1.5 cm by the running gel and fixed with 45% methanol/water containing 5% acetic acid for 20 min. The fixed gel was washed with 50% methanol/water and water, and manually cut into 8 gel slices without gel staining. The excised gels were subjected to in-gel digestion using trypsin (In-Gel Tryptic Digestion Kit, Thermo Fisher Scientific, trypsin 200 ng/slice). The eluted peptide solution from the gel was freeze-dried and redissolved with 18 μL of 2% CH<sub>3</sub>CN/water containing 0.1% TFA. The solutions (4.0 μL) were subjected to LC–MS analyses. Three independent SILAC experiments were performed, in which proteins detected at least twice with paired light- and heavy-labeled peptides were included in the data sets as identified proteins.

**LC–MS Analysis.** After proteome labeling, proteins were digested with trypsin in solution or in gel. The samples for protein identification were analyzed by nanoflow reverse phase liquid chromatography followed by tandem MS, using a LTQ-Orbitrap XL hybrid mass spectrometer (Thermo Fisher Scientific). For LTQ-Orbitrap XL, a capillary reverse phase HPLC–MS/MS system composed of an Agilent 1100 series gradient pump equipped with Valco C2 valves with 150-μm ports, and LTQ-Orbitrap XL hybrid mass spectrometer equipped with an XYZ nanoelectrospray ionization (NSI) source (AMR). Samples were automatically injected using PAL system (CTC analytics, Zwilling, Switzerland) into a peptide L-trap column OSD (5 μm, AMR) attached to an injector valve for desalinating and concentrating peptides. After washing the trap with MS-grade water containing 0.1% trifluoroacetic acid and 2% acetonitrile (solvent C), the peptides were loaded into a nano HPLC capillary column (C18-packed with the gel particle size of 3 μm, 0.1 × 150 mm, Nikkyo Technos) by switching the valve. The eluents used were: A, 100% water containing 0.1% formic acid, and B, 80% acetonitrile containing 0.1% formic acid. The column was developed at a flow rate of 200–500 nL/min with the concentration gradient of acetonitrile. Xcalibur 2.1 system (Thermo Fisher Scientific) was used to record peptide spectra over the mass range of  $m/z$  350–1500, and MS/MS spectra in information-dependent data acquisition over the mass range of  $m/z$  150–2000. Repeatedly, MS spectra were recorded followed by three data-dependent collision induced dissociation (CID) MS/MS spectra generated from three or eight highest intensity precursor ions for the nonquantitative MS or SILAC experiment, respectively. Multiple charged peptides were chosen for MS/MS experiments due to their good fragmentation characteristics. MS/MS spectra were interpreted and peak lists were generated by Proteome Discoverer 1.4 (Thermo Fisher Scientific). Searches were performed by using the SEQUEST-HT (Thermo Fisher Scientific) against uniprot database. Dynamic modifications of Et4-Rhod, carbamidomethylation on cysteine and oxidation on methionine were searched with peptide mass tolerance at 10 or 20 ppm for nonquantitative MS or SILAC experiment, respectively; MS/MS mass tolerance of 0.6 Da. Multiple Et4-Rhod modified peptides were omitted from the data sets. The resultant data set was filtered to a maximum false discovery rate (FDR) of 0.01. Identified peptides with same sequence were counted as the identical peptides.

## ■ ASSOCIATED CONTENT

### ● Supporting Information

The Supporting Information is available free of charge on the ACS Publications website at DOI: 10.1021/jacs.6b02254.

Supporting Figures, Tables, and Methods. (PDF)

Supplementary Data S1. (XLSX)

Supplementary Data S2. (XLSX)

Supplementary Data S3. (XLSX)

Supplementary Data S4. (XLSX)

Supplementary Data S5. (XLSX)

Supplementary Data S6. (XLSX)

## ■ AUTHOR INFORMATION

### Corresponding Author

\*ihamachi@sbchem.kyoto-u.ac.jp

### Notes

The authors declare no competing financial interest.

## ■ ACKNOWLEDGMENTS

We thank Nozomi Ogawa, Karin Nishimura and Youhei Tatsukami (Kyoto University) for experimental support of LC–MS and helpful discussion. We also thank Sho Wakayama (Kyoto University) for preparation of brain slices. Y.Y. (26-4745) is supported by Japan Society for the Promotion of Science (JSPS) for doctoral fellowships. This work was funded by the Japan Science and Technology Agency (JST) Core Research for Evolutional Science and Technology (CREST) and by JSPS KAKENHI (15H01637) to I.H.

## ■ REFERENCES

- (1) (a) Yates, J. R. *J. Am. Chem. Soc.* **2013**, *135*, 1629. (b) Aebersold, R.; Mann, M. *Nature* **2003**, *422*, 198. (c) Iwasaki, M.; Ishihama, Y. *Chromatography* **2014**, *35*, 73.
- (2) (a) Weerapana, E.; Wang, C.; Simon, G. M.; Richter, F.; Khare, S.; Dillon, M. B. D.; Bachovchin, D. a; Mowen, K.; Baker, D.; Cravatt, B. F. *Nature* **2010**, *468*, 790. (b) Woo, C. M.; Iavarone, A. T.; Spicciarich, D. R.; Palaniappan, K. K.; Bertozzi, C. R. *Nat. Methods* **2015**, *12*, 561. (c) Hayashi, T.; Sun, Y.; Tamura, T.; Kuwata, K.; Song, Z.; Takaoka, Y.; Hamachi, I. *J. Am. Chem. Soc.* **2013**, *135*, 12252. (d) Li, X.; Foley, E. a; Molloy, K. R.; Li, Y.; Chait, B. T.; Kapoor, T. M. *J. Am. Chem. Soc.* **2012**, *134*, 1982. (e) Lin, S.; Zhang, Z.; Xu, H.; Li, L.; Chen, S.; Li, J.; Hao, Z.; Chen, P. R. *J. Am. Chem. Soc.* **2011**, *133*, 20581.
- (3) (a) Liu, Y.; Patricelli, M. P.; Cravatt, B. F. *Proc. Natl. Acad. Sci. U. S. A.* **1999**, *96*, 14694. (b) Cravatt, B. F.; Wright, A. T.; Kozarich, J. W. *Annu. Rev. Biochem.* **2008**, *77*, 383.
- (4) Nunnari, J.; Suomalainen, A. *Cell* **2012**, *148*, 1145.
- (5) Drissi, R.; Dubois, M. L.; Boisvert, F. M. *FEBS J.* **2013**, *280*, 5626.
- (6) (a) Rhee, H.-W.; Zou, P.; Udeshi, N. D.; Martell, J. D.; Mootha, V. K.; Carr, S. A.; Ting, A. Y. *Science* **2013**, *339*, 1328. (b) Hung, V.; Zou, P.; Rhee, H.-W.; Udeshi, N. D.; Cracan, V.; Svinkina, T.; Carr, S. A.; Mootha, V. K.; Ting, A. Y. *Mol. Cell* **2014**, *55*, 332.
- (7) Most recently, APEX strategy has been successfully applied to *Drosophila* tissue samples: Chen, C. L.; Hu, Y.; Udeshi, N. D.; Lau, T. Y.; Wirtz-Peitz, F.; He, L.; Ting, A. Y.; Carr, S. A.; Perrimon, N. *Proc. Natl. Acad. Sci. U. S. A.* **2015**, *112*, 12093.
- (8) Washbourne, P.; McAllister, a. K. *Curr. Opin. Neurobiol.* **2002**, *12*, 566.
- (9) Ward, J. F.; Evans, J. W.; Limoli, C. L.; Calabro-Jones, P. M. *Br. J. Cancer. Suppl.* **1987**, *8*, 105.
- (10) (a) Wiedner, S. D.; Anderson, L. N.; Sadler, N. C.; Chrisler, W. B.; Kodali, V. K.; Smith, R. D.; Wright, A. T. *Angew. Chem., Int. Ed.* **2014**, *53*, 2919. (b) Yang, P.-Y.; Liu, K.; Zhang, C.; Chen, G. Y. J.; Shen, Y.; Ngai, M. H.; Lear, M. J.; Yao, S. Q. *Chem. - Asian J.* **2011**, *6*, 2762.
- (11) Yasueda, Y.; Tamura, T.; Hamachi, I. *Chem. Lett.* **2016**, *45*, 265.
- (12) (a) Sletten, E. M.; Bertozzi, C. R. *Angew. Chem., Int. Ed.* **2009**, *48*, 6974. (b) Takaoka, Y.; Ojida, A.; Hamachi, I. *Angew. Chem., Int. Ed.* **2013**, *52*, 4088.
- (13) (a) Hoye, A. T.; Davoren, J. E.; Wipf, P.; Fink, M. P.; Kagan, V. E. *Acc. Chem. Res.* **2008**, *41*, 87. (b) Rin Jean, S.; Tulumello, D. V.; Wisnovsky, S. P.; Lei, E. K.; Pereira, M. P.; Kelley, S. O. *ACS Chem. Biol.* **2014**, *9*, 323. (c) Wu, S.; Song, Y.; Li, Z.; Wu, Z.; Han, J.; Han, S. *Anal. Methods* **2012**, *4*, 1699.

- (14) (a) Weerapana, E.; Simon, G. M.; Cravatt, B. F. *Nat. Chem. Biol.* **2008**, *4*, 405. (b) Son, J.; Lee, J.; Lee, J.; Schu, A.; Chang, Y. *ACS Chem. Biol.* **2010**, *5*, 449.
- (15) Sadler, N. C.; Melnicki, M. R.; Serres, M. H.; Merkley, E. D.; Chrisler, W. B.; Hill, E. A.; Romine, M. F.; Kim, S.; Zink, E. M.; Datta, S.; Smith, R. D.; Beliaev, A. S.; Konopka, A.; Wright, A. T. *ACS Chem. Biol.* **2014**, *9*, 291.
- (16) (a) Wang, H.; Koshi, Y.; Minato, D.; Nonaka, H.; Kiyonaka, S.; Mori, Y.; Tsukiji, S.; Hamachi, I. *J. Am. Chem. Soc.* **2011**, *133*, 12220. (b) Greenwald, R. B.; Pendri, A.; Martinez, A.; Gilbert, C.; Bradley, P. *Bioconjugate Chem.* **1996**, *7*, 638.
- (17) Shannon, D. A.; Weerapana, E. *Curr. Opin. Chem. Biol.* **2015**, *24*, 18.
- (18) (a) Gu, C.; Shannon, D. A.; Colby, T.; Wang, Z.; Shabab, M.; Kumari, S.; Villamor, J. G.; McLaughlin, C. J.; Weerapana, E.; Kaiser, M.; Cravatt, B. F.; van der Hoorn, R. A. L. *Chem. Biol.* **2013**, *20*, 541. (b) Narayanan, A.; Jones, L. H. *Chem. Sci.* **2015**, *6*, 2650.
- (19) Sakurai, K.; Ozawa, S.; Yamada, R.; Yasui, T.; Mizuno, S. *ChemBioChem* **2014**, *15*, 1399.
- (20) Emaus, R. K.; Grunwald, R.; Lemasters, J. J. *Biochim. Biophys. Acta, Bioenerg.* **1986**, *850*, 436.
- (21) Gao, W.; Pu, Y.; Luo, K. Q.; Chang, D. C. *J. Cell Sci.* **2001**, *114*, 2855.
- (22) Campanella, M.; Seraphim, A.; Abeti, R.; Casswell, E.; Echave, P.; Duchen, M. R. *Biochim. Biophys. Acta, Bioenerg.* **2009**, *1787*, 393.
- (23) The selectivity and enrichment efficiency of our homemade anti-Et4-Rhod antibody (antiserum) were revealed in [Figure S8](#).
- (24) (a) Adam, G. C.; Burbaum, J.; Kozarich, J. W.; Patricelli, M. P.; Cravatt, B. F. *J. Am. Chem. Soc.* **2004**, *126*, 1363. (b) Masuda, T.; Tomita, M.; Ishihama, Y. *J. Proteome Res.* **2008**, *7*, 731.
- (25) Kiefer, F.; Arnold, K.; Künzli, M.; Bordoli, L.; Schwede, T. *Nucleic Acids Res.* **2009**, *37*, 387.
- (26) Since the MRM-based labeling follows the intermolecular reaction mechanism, high-abundance proteins tend to be more labeled and enriched, while low-abundance proteins can also be labeled enough to be identified (see [Figure S11](#)).
- (27) It is reported that Rhodamine derivatives mainly distribute into the mitochondria matrix (see reference 20).
- (28) Marini, E. S.; Giampietri, C.; Petrunaro, S.; Conti, S.; Filippini, A.; Scorrano, L.; Ziparo, E. *Cell Death Differ.* **2015**, *22*, 1131.
- (29) Zhang, H.; Wang, Y.; Li, J.; Yu, J.; Pu, J.; Li, L.; Zhang, H.; Zhang, S.; Peng, G.; Yang, F.; Liu, P. *J. Proteome Res.* **2011**, *10*, 4757.
- (30) Proteins identified as “nonmitochondrial proteins” include 25 cytoskeletal proteins.
- (31) (a) Calvo, S. E.; Clauser, K. R.; Mootha, V. K. *Nucleic Acids Res.* **2016**, *44*, D1251. (b) Pagliarini, D. J.; Calvo, S. E.; Chang, B.; Sheth, S. A.; Vafai, S. B.; Ong, S.-E.; Walford, G. A.; Sugiana, C.; Boneh, A.; Chen, W. K.; Hill, D. E.; Vidal, M.; Evans, J. G.; Thorburn, D. R.; Carr, S. A.; Mootha, V. K. *Cell* **2008**, *134*, 112.
- (32) Huang, D. W.; Sherman, B. T.; Lempicki, R. A. *Nat. Protoc.* **2009**, *4*, 44.
- (33) (a) Ong, S. E.; Mann, M. *Nat. Protoc.* **2006**, *1*, 2650. (b) Bantscheff, M.; Schirle, M.; Sweetman, G.; Rick, J.; Kuster, B. *Anal. Bioanal. Chem.* **2007**, *389*, 1017.
- (34) (a) Fei, Q.; McCormack, A. L.; Di Monte, D. A.; Ethell, D. W. *J. Biol. Chem.* **2008**, *283*, 3357. (b) Takeyama, N.; Tanaka, T.; Yabuki, T.; Nakatani, T. *Int. J. Toxicol.* **2004**, *23*, 33.
- (35) (a) Park, K. J.; Kim, Y. J.; Kim, J.; Kim, S. M.; Lee, S. Y.; Bae, J. W.; Hwang, K. K.; Kim, D. W.; Cho, M. C. *Korean Circ. J.* **2012**, *42*, 23. (b) Lu, W.; Fu, Z.; Wang, H.; Feng, J.; Wei, J.; Guo, M. *Mol. Cell. Biochem.* **2014**, *387*, 261. (c) De Haan, J. B.; Bladier, C.; Griffiths, P.; Kelner, M.; O’Shea, R. D.; Cheung, N. S.; Bronson, R. T.; Silvestro, M. J.; Wild, S.; Zheng, S. S.; Beart, P. M.; Hertzog, P. J.; Kola, I. *J. Biol. Chem.* **1998**, *273*, 22528.
- (36) (a) Choi, J. W.; Song, M.-Y.; Park, K.-S. *Mol. Biosyst.* **2014**, *10*, 1940. (b) Ricci, J. E.; Muñoz-Pinedo, C.; Fitzgerald, P.; Bailly-Maitre, B.; Perkins, G. A.; Yadava, N.; Scheffler, I. E.; Ellisman, M. H.; Green, D. R. *Cell* **2004**, *117*, 773. (c) Impheng, H.; Pongcharoen, S.; Richert, L.; Pektong, D.; Srisawang, P. *PLoS One* **2014**, *9*, e107842.
- (37) Hangen, E.; Blomgren, K.; Bénit, P.; Kroemer, G.; Modjtahedi, N. *Trends Biochem. Sci.* **2010**, *35*, 278.
- (38) (a) Karp, C. M.; Pan, H.; Zhang, M.; Buckley, D. J.; Schuler, L. A.; Buckley, A. R. *Cancer Res.* **2004**, *64*, 1016. (b) Karp, C. M.; Shukla, M. N.; Buckley, D. J.; Buckley, A. R. *Oncogene* **2007**, *26*, 1780.
- (39) (a) Keane, P. C.; Kurzawa, M.; Blain, P. G.; Morris, C. M. *Parkinson’s Dis.* **2011**, *2011*, 716871. (b) Keeney, P. M. *J. Neurosci.* **2006**, *26*, 5256. (c) McKenzie, M.; Ryan, M. T. *IUBMB Life* **2010**, *62*, 497. (d) Mimaki, M.; Wang, X.; McKenzie, M.; Thorburn, D. R.; Ryan, M. T. *Biochim. Biophys. Acta, Bioenerg.* **2012**, *1817*, 851.
- (40) (a) Bota, D. A.; Davies, K. J. A. *Nat. Cell Biol.* **2002**, *4*, 674. (b) Goard, C. A.; Schimmer, A. D. *Oncogene* **2014**, *33*, 2690.
- (41) Calvo, S. E.; Mootha, V. K. *Annu. Rev. Genomics Hum. Genet.* **2010**, *11*, 25.
- (42) Notably, the mitochondrial-surface specific fluorescent probe was recently developed by Uesugi and coworkers: Kawazoe, Y.; Shimogawa, H.; Sato, A.; Uesugi, M. *Angew. Chem., Int. Ed.* **2011**, *50*, 5478.